Multifrequency ESR analysis of the E'_δ defect in a-SiO_2

M. Jivanescu, A. Stesmans, and V. V. Afanas'ev
Semiconductor Physics Laboratory, Department of Physics and Institute for Nanoscale Physics and Chemistry (INPAC), University of Leuven, Celestijnenlaan 200 D, B-3001 Leuven, Belgium
(Received 13 August 2010; published 16 March 2011)

A multifrequency (X, K, Q band) electron spin resonance (ESR) study has been carried out on the nature of the E'_δ defect in vitreous (v) SiO_2, both at cryogenic and room temperature (T), using two detection modes on six types of commercial v-silica subjected to three kinds of irradiation [UV, vacuum ultraviolet (VUV), and ^{60}Co γ photons]. The E'_δ signal could be generated only in three types of v-SiO_2, and only, yet always, by two types of irradiation, VUV and ^{60}Co γ rays—not UV—suggesting that the E'_δ activation starts predominantly from preexisting sites through ionization processes. The inferred intensity ratio of the resolved ^{29}Si hyperfine (hf) structure to the central Zeeman signal is found to reassuringly coincide over the observational frequencies and T's studied. The as-inferred average value (≈20.3%) alone would point to hf interaction of the unpaired spin with $n = 4$ equivalent Si sites, confirming the center's delocalized nature as initially proposed. Yet, with the inclusion of previous experimental experience, the $n = 5$ case cannot be excluded, and in fact, should be given full consideration as well. In line with the previous conclusion, the result decisively refutes the recurrent theoretically propagated positively charged Si dimer (Si_2) model, thus urging discontinuation of the use of the Si_2 label for the E'_δ center. In fact, none of the thus-far advanced atomic models may apply, as all are theoretically projected to essentially correspond to $n = 1(2)$ cases due to limited spin delocalization. Extrinsic Al-related defects ($[AlO_4]^0$, Al E') are co-observed, where a noteworthy finding is that the E'_δ is only observed in those (3) v-silica also showing the Al E' center, possibly Na^+ compensated, in the initial γ-irradiated state. This may signify some indirect role of charge compensators in activating/stabilizing E'_δ centers, which may need incorporation to further theoretical modeling. The exposed T independence of the ESR parameters, including hf, refers to an electronically rigid structure with no dynamical readjustment process occurring in the range $T \geqslant 4.2$ K. The experimental absence of the theoretical Si_2 defect is discussed within the context of its projected closely isospectral ESR appearance to the E'_δ signal.

DOI: 10.1103/PhysRevB.83.094118 PACS number(s): 61.82.Ms, 68.35.Dv, 76.30.−v, 31.30.Gs

I. INTRODUCTION

Driven by its impressive set of superb physical and chemical properties, SiO_2, in various forms, has provided over history many highly functional applications. To name a few, they range from it being the basic material for low-loss optical fiber waveguides to serving for decades as the basic, still superior, high quality gate insulator in Si-based electronic devices—the famous thermally grown Si/SiO_2 entity;[1] it has made amorphous (a)-SiO_2 probably the most studied oxide so far.

By their nature, various physical properties are to some extent affected by structural imperfections, such as point defects. In the case of optical fibers, they may unacceptably impair photonic transport through optical absorption,[2] while in the case of SiO_2 serving as a gate insulator in complementary metal-oxide-semiconductor (MOS) devices, defects may behave as detrimental charge traps, thus deteriorating the performance of MOS devices.[3]

A particular class here is comprised of the intrinsic O-vacancy related point defects in silica, referred to as the family of E' centers as detected by electron spin resonance (ESR). This technique has proven to be a most adequate tool for point defect investigation of SiO_2 since 1956, when Weeks[4] first reported a paramagnetic center in neutron-bombarded quartz and fused silica, termed E'_γ. By drawing dry a-SiO_2 into fibers, defects identical[5] to the ones created by irradiation are produced, that is, Si−O or preexisting Si−Si bonds can break and result in E' center creation,[6] i.e., mechanically induced atomic rearrangement (disruption).

From extensive experimental ESR and theoretical studies, the generic entity[7] of the E' class of defects has been identified as the threefold coordinated Si entity ($O_3{\equiv}Si^\bullet$, the dot representing an unpaired electron in a sp^3-like orbital) at the site of an O vacancy. There are different variants both in crystalline (c-)quartz (E'_1, E'_2, E'_4, ...) and a-SiO_2 (E'_α, E'_β, E'_γ, E'_δ, and E'_s) with properties reviewed in several comprehensive works.[8–11] While several centers are accepted to be reliably atomically identified, the definite atomic nature of (at least) one variant observed in a-SiO_2, E'_δ, is still elusive.[12]

In the search for atomic identification, a key role is played by resolved ESR hyperfine (hf) structure, E'_δ showing one hf doublet of splitting ∼100 G to be compared with ≈420 G for the "strong" doublet (hf doublet with largest splitting) of the E'_γ center. No counterpart center has so far been reported in c-quartz nor has the E'_δ been observed in standard thermal oxide. Besides the particular hf structure and the magnitude of measured hf splitting (hfs), correct atomic modeling hinges on the knowledge of the correct relative intensities of observed hf signals, which, unlike the E'_γ case,[7] is still a subject of dispute[12] for E'_δ.

The E'_δ point defects were concluded to have a detrimental effect on device performance,[13,14] the defects being observed in buried oxides as well as in bulk silica. Over the 25 years since its discovery,[15] four atomic models have been proposed (in fact

only three, if excluding impurity involvement), all based on a central unpaired sp^3 Si orbital. In shorthand, we will designate these as Si_n ($n = 2, 4, 5$) models according to the number n of (equivalent) Si atom sites forming the immediate defect core over which the unpaired electron is mainly delocalized (*vide infra*). Yet, no model could so far unambiguously be assigned.[12,16,17]

The scope of the current work is to address the E'_δ hf structure in pertinent detail through a broad multifrequency continuous wave (cw) ESR study carried out at both low and high temperature (T). In this way, it is intended to compile a statistically meaningful and extended set of data on the relative intensity of the resolved ^{29}Si hf structure (i.e., equivalent Si sites involved) inferred through orthodox unsaturated cw first-harmonic mode ESR absorption spectroscopy, with a main goal to provide a solid ground for decisive E'_δ atomic modeling. As a major finding, the results point to a 4(5)-Si site delocalization shell, thus clearly refuting the Si_2 (dimer) model, in line with a previous experimental conclusion.[17]

Relatedly, within the context of the presumed (singly) positive charge state of the E'_δ when ESR active,[14,18–20] attention is paid to the possible influence in E'_δ appearance of charge compensator units, revealing a potential correlation with co-present Al E' centers. The results are discussed within the current state of theoretical modeling.

In the next section we discuss the known salient E'_δ properties relevant for the current study, as obtained mainly from ESR experimenting and theoretical work. Experimental details are presented in Sec. III, followed by the presentation of the results and interpretation. After discussion of the results in Sec. V, conclusions and final remarks are given in Sec. VI.

II. ESR WORK AND CURRENT THEORETICAL INSIGHT

The E'_δ defect was first reported by Griscom and Friebele[15] in 1986, when studying by X-band ESR as a function of isochronal annealing the influence of different 100-keV x-ray irradiation doses applied at 77 K on plasma deposited Cl-rich synthetic O-deficient (type IV) silicas of low OH content. The E'_δ signal was observed as an almost isotropic, narrow signal of peak-to-peak width $\Delta B_{pp} \approx 0.65$ G and a zero crossing value $g_c \sim 2.0020$ (i.e., principal g values inferred as $g_1 = 2.0018$, $g_2 = g_3 = 2.0021$, referring to axial symmetry), with an associated strong hf doublet split by ≈100 G where the correlated nature of the hf doublet was concluded from the similar activation and bleaching behavior as the main central Zeeman line. This has been confirmed in later work.[17,21] Because the defect appears to share one principal g value (g_1) with the "traditional" E'-type centers (E'_α, E'_γ), it has been adopted as another species of the E' defect family dubbed the δ variant. In that work, though, the intensity of the E'_δ associated hf doublet appeared too small to enable proper detection in the unsaturated first-harmonic ESR mode. Yet based on its observed similar saturation behavior as E'_γ, considerations about relative ESR signal intensities were carried out based on comparison of observed *amplitudes* (heights) of first-derivative spectra of the central Zeeman signals and high power second-harmonic out-of-phase hf spectra—a not-straightforward procedure (see below). For annealing above ≈200 °C, the heights of the 100-G doublets were found to correlate well with the amplitude of the E'_δ central line. The observed hf splitting of ≈100 G associated with E'_δ is about one-fourth of the average ≈418–420 G splitting of the primary E'_γ hf doublet,[7,11] which can be envisioned as resulting from the E'_δ electron being delocalized over several (four) Si atoms. This finding, together with the nearly isotropic property in addition to the presumed involvement of Cl impurities in the atomic structure, led to the idea of a *delocalized* E'-type defect:[15] the E'_δ center was tentatively modeled as a SiO_4 vacancy dressed with three Cl atoms, with the unpaired spin delocalized over four Si atoms. Thus its precursor is seen as a SiO_4 vacancy decorated by four Cl atoms bonded to the four Si atoms (Si_4:Cl_4 model), from where a Cl atom has been removed by irradiation.

Besides atomic chlorine, another defect initially observed in this work was a triplet state (electron spin $S = 1$; $g_c \approx 2.00$) biradical, with an associated signal observed at half the resonance field ($g_c \approx 4$) of the E'_δ centers. The appearance in the same materials and the similar response to annealing and irradiation indicated a correlation between the occurrence of the $S = 1$ state and E'_δ defects referring to similar precursor structures at their origin. Accordingly, this $S = 1$ defect was modeled as an SiO_4 vacancy, now decorated by only two Cl ions, wherein two unpaired spins are localized in dangling sp^3 orbitals at different Si atoms of the cavity. The signal is removed[15] by a 10-min anneal at $T \geqslant 200$ °C.

From X-band ESR studies of the influence of ^{60}Co γ irradiation on a variety of high-purity bulk a-SiO_2 samples, both before and after room temperature (RT) and 500 °C treatments in H_2, Tohmon *et al.*[22] concluded that Cl is not a prerequisite (and neither F) for E'_δ center formation. Yet, from correlated infrared absorption measurements, they concluded the necessity of O deficiency, from where it was advanced E'_δ to be an O-deficient center. So, with no impurity involvement, they suggested as an alternative model an ionized single O vacancy with the unpaired electron rather evenly delocalized over the two neighboring Si atoms (Si_2; a charged Si−Si dimer), as pictured in Fig. 1(a) for the positive charge state. In the same scheme, the concomitantly observed triplet state ($S = 1$) defect was assigned to two neighboring E'_γ centers (≡Si$^\bullet$ $^\bullet$Si≡) with the two unpaired electrons having the same spin direction.

In a later extensive ESR study on Si/SiO_2 device structures,[18] Vanheusden and Stesmans observed E'_δ centers in buried Si oxides (BOX) in (100)Si, fabricated using the separation by implantation of oxygen (SIMOX) technique, the virtually Cl- and F-free nature of these SIMOX oxides herewith directly disqualifying these impurities as a key part of the E'_δ structure. The center is observed after ^{60}Co γ irradiation,[23] yet even more clearly after exposure of the BOX to cathodic dc glow discharge Ar plasma treatment.[18,24] Pertinently, as to the latter Ar activation procedure, the E'_δ signal drops drastically after 10-min vacuum anneal at 200 °C, and could not be observed after reoxidation of the BOX nor, as expected, in conventional thermally grown oxide, pointing to E'_δ defect generation from specific precursor sites. It was also observed that the highest E'_δ density is obtained in the cathodic Ar bombardment configuration,[18] indicative of a positively charged point defect, *a hole trap*, in agreement with other work[14,19,20] where carrier injection and charging experiments

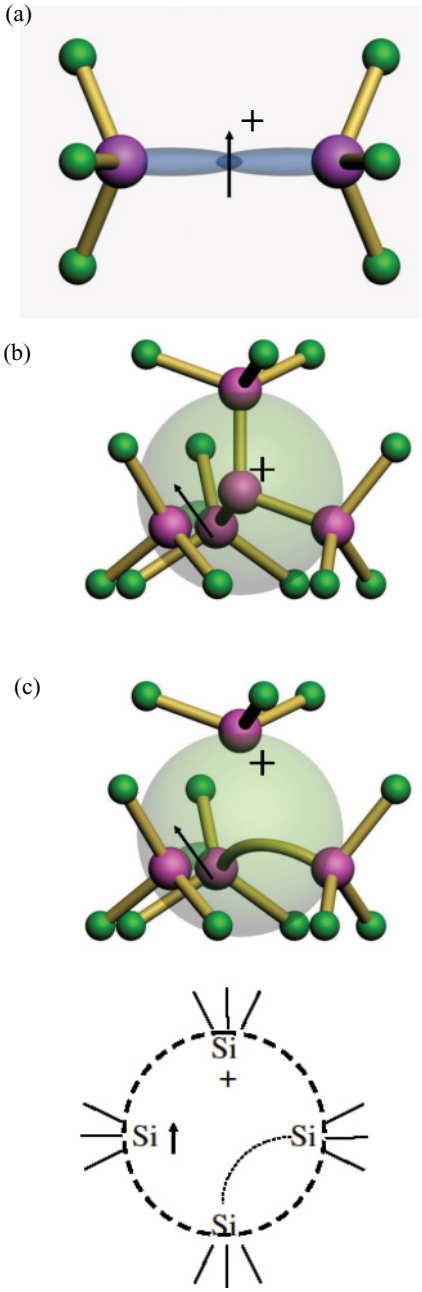

FIG. 1. (Color online) Ball-and-stick pictures of the intrinsic models proposed for the E'_δ defect: (a) Si_2 dimer model where the unpaired electron-spin density is predominantly delocalized between the two neighboring Si atoms, each backbonded to three oxygens of the SiO_2 matrix. (b) Si_5 tetrahedral Si-cluster model where the overshadowing sphere suggests electron-spin delocalization over the cluster. (c) Si_4 cluster model with added two-dimensional schematic. The dotted bow suggests dynamic (weak) bond formation. As denoted, all three models in the ESR active state represent a net charge of +1. Large and small spheres represent Si and O-atoms, respectively.

were carried out in combination with ESR. Moreover, depth profiling indicated enhanced E'_δ generation in regions of an enhanced excess of Si, i.e., in the BOX layers near the interface ($\lesssim$20 nm) with the Si substrate, unlike E'_γ centers, which are produced more uniformly over the BOX. The results led to the proposal of an alternative E'_δ microstructure based on the existence of Si clusters, more precisely, the presumably positively charged Si_5 [see Fig. 1(b)] model where the unpaired electron delocalizes additionally over the four Si atoms (perhaps) tetrahedrally configured around the central Si atom; this may be viewed basically as a SiO_4 vacancy substituted by a single Si atom, or four O vacancies clustered around a Si atom, or Si "tetrahedron." Part of the interpretation had arisen from the consideration of the particular way BOX is manufactured. Unlike the commonly studied vitreous silica glasses[10,15] (i.e., fused natural quartz, synthetic silica prepared by methods such as flame hydrolysis and plasma deposition, all involving in principle free oxidation of Si) as also addressed in the current work, BOX is formed[18] by implantation of a high dose ($\geqslant 10^{18}$ cm^{-2}) of high-energy (100–200 keV) O^+ ions into a *c*-Si target kept above about 550 °C. This results in a confined (stressed) *Si-enriched* oxide buried underneath a superficial *c*-Si layer.

In a related ESR work[25] comparing the generation of E'_δ centers in BOX by different methods, it was found that while energetic photons (X,γ) and ion bombardment activate the usual E'_δ center of (albeit weak) axial symmetry of $g_c \approx 2.0019$, hole injection combined with VUV excitation results in the generation of a (highly) isotropic type of $g_c \approx 2.0021$, termed $E'_{\delta 2}$. It indicated the E'_δ generation to be damage-agent specific. The E'_δ signal is also observed to bleach over time in room ambient (over about one day after hole injection; about weeks after dc glow discharge).

Zvanut *et al.*[26] observed E'_δ center formation in x-ray irradiated BOX. The latter was prepared either by thermally growing a thin oxide layer on Si and subsequent overlaying by polycrystalline Si followed by an annealing step, or by the SIMOX method, indicating that the initial oxide fabrication technique is not determining on its own the defect generation. Here, it rather appears to be the burying (O-deficient) aspect in combination with the post oxide formation applied thermal steps affecting the ultimate degree of oxygen deficiency attained. As interpreted, out-diffusion of oxygen from the silica[27,28] layer as volatile SiO molecules[26] created by the reaction of SiO_2 with Si (from the coating layer) during the high-T anneal is creating an O-deficient zone accommodating the E'_δ precursors. In fact, it resembles much the effect of the high-temperature annealing ($T_{an} = 1130$ °C) in O-free ambient of ≈66-nm-thick thermally grown *a*-SiO_2 on (100) *p*-Si, leading to E'_δ generation.[29]

As mentioned, in ESR-based point defect identification, spectral hf structure plays a crucial role, to such extent that no defect can be considered reliably atomically modeled if not supported by insightfully assigned spectral hf properties, underpinned by theory. This includes hf spectral structure, hf splitting and, not the least, the relative intensity ratio of respective signals, the latter reflecting the distribution of the unpaired electron wave function (spin density) over the defect's constituent atoms. And, when limited by ESR sensitivity, this has not always been paid sufficient attention to. The ratio $R_{hf}(\eta, n)$ of the intensity of a hf multiplet (I_{hf}) to that of the central main (Zeeman) signal (I_c) is a function of η, the natural abundance of the hf-originating nuclear isotope, and n, the number of such atoms in a shell of equivalent atom sites that the unpaired spin is interacting with. With η known, n provides a basic clue to the defect structure. Invariably, the correct

orthodox way to determine signal intensities (area under the absorption curve $\propto\chi''$) is by nonsaturation conventional first-harmonic ESR spectroscopy. But when in lack of sensitivity or overwhelmed by hard-to-disentangle overlapping signals, it is tempting to turn[15,21] to the high power second-harmonic phase-quadrature detection mode (saturation spectroscopy), which has been shown empirically to be generally a much more sensitive means to resolve hf structure for point defects in silica and oxides,[11,30,31] among others, due to the high saturability of such defects. Under appropriate experimental conditions for a certain defect, the second-harmonic saturation spectra appear identical to the direct absorption shapes (χ''), as evidenced empirically.[30,31] So, in principle, besides revealing spectral composition, the former spectroscopy may be conveniently used for signal line-shape analysis. However, the intensity of second-harmonic spectra depends in a complex manner on the defect relaxation times as well as on various experimental parameters such as modulation frequency and amplitude, and applied microwave frequency (f_μ) and power, befogging quantitative analysis. Some means of independent calibration is required.

Using *X*-band ESR, Zhang and Leisure[21] addressed the hf structure of E'_δ centers generated by x-ray irradiation in high-purity silicas synthesized by chemical vapor deposition (CVD) which allows impurity and moisture control. They observed E'_δ signals as well as an interconversion between E'_γ and E'_β centers depending on anneal treatment. As a major result, these authors were first to determine $R_{\rm hf}$ for E'_δ giving $R_{\rm hf} = 0.175 - 0.191$, from where the value $n = 4$ was extracted. While rejecting the Si_2 atom model, this led to the proposal of the revised model for E'_δ as being a $[SiO_4]^+$ vacancy (Si_4 model; two strained nearby O-vacancy centers), i.e., essentially the initial Griscom and Friebele[15] model with no Cl (impurity) involvement, as depicted in Fig. 1(c). Pertinently, one more point to be noted is the difference in net charge state, that is, 0 and +1 for the initial and revised models, respectively. Based on the $n = 4$ result, also the Si_5 model was deemed untenable, adding that it is highly unlikely that such clusters would be present in the studied fused silica.

The three models, Si_2, Si_4, and Si_5, thus proposed for E'_δ have been evaluated by Chavez *et al.*[32] and Karna *et al.*[33] using first-principles quantum-mechanical calculations concluding that the E'_δ center is a symmetric variant of E'_γ, i.e., symmetrically relaxed O monovacancy—the positively charged Si dimer center (Si_2). In α-quartz, it is known as the short Si-Si distance (~2.7 Å) variant[34,35] of E'_1 in near-perfect crystal (NPC) equilibrium symmetry.[34] Its properties have been addressed in various theoretical works.[12,32–34,36,37]

The E'_δ hf structure consists of a single doublet of which, as turns out, the splitting is physically determined by the isotropic Fermi-contact part[38] generally given as $a_{\rm iso} = \frac{2}{3}\mu_0 g_N \beta_N g_e \beta |\psi_S(0)|^2$, where g_N and g_e are the nuclear and electron g factors, β_N and β are the nuclear and Bohr magneton, and μ_0 is the vacuum permeability; $|\psi_S(0)|^2$ is the unpaired spin density (s part) at the interacting nuclei, here ascribed to ^{29}Si isotopes (nuclear spin $I = \frac{1}{2}$;$\eta = 4.67\%$). Most pertinently, spin-density calculations[32] indicate that the unpaired electron would not be delocalized over the entire cluster but preferentially on a *single* Si atom in the case of the "Si_5" model or over (between) a *single pair* of Si atoms for the other two cases, reducing the s-orbital contribution on the Si nuclei. The symmetry reduction of the electronic wave function when considering the Si_4 and Si_5 tetrahedral clusters was attributed to a dynamic Jahn-Teller effect. Molecular calculations[37] show that the main difference between the positively charged E'_δ and E'_γ point defects is reflected in the distance between the two constituent Si atoms: if the Si-Si distance is small enough, the two potential wells combine into a single one and an E'_δ center is obtained.

The E'_δ defect has initially been associated with the Si_2 dimer on the basis of the calculated hf splitting of 100–135 G.[32,39] It has since been supported by various theoretical works.[12,36] The E'_δ center has been described as a metastable nonpuckered form of E'_γ, the latter being perhaps a few tenths of meV more stable. But as to a-SiO_2, this is still in dispute.[40,41] Other theoretical work[42] has concluded that the positively charged Si dimer is the stable configuration for about 80% of the O vacancy sites. Later work[43] addressing spectroscopic aspects of E'_δ has calculated the principal g matrix values ($g_1 = 2.0018$, $g_2 = 2.0034$, $g_3 = 2.0043$), which are found in good agreement with initial experimental results[15] ($g_1 = 2.0018$, $g_2 = g_3 = 2.0021$). The optical absorption energy for E'_δ was calculated as 6.33 eV, to be compared with the known value of 5.8 eV for E'_γ.

In recent theoretical work,[12] Tuttle and Pantelides studied Si clusters in a-SiO_2 described as arising from vacancy clusters, $n(V_O)$, with n in the range 1–7. Noteworthy inferences include the following: (i) Based on the calculation of the formation energy per Si−Si bond, it is found that the Si_5 cluster (four O-vacancy cluster) is the most stable, significantly (~0.23 eV per Si−Si bond) more favorable to form than the Si_2 dimer. Yet, while theory would thus favor V_O clustering, its predominant formation was considered not to become necessarily expressed in practice due to the silica growth conditions. (ii) For the various clusters considered, comparable isotropic hf values are found, given as ~100 G for Si_2, with a somewhat broader range of 80–120 G for the Si_5 model. In essence on this matter, the latter is thus found effectively to correspond to a $n = 2$ case, in line with previous work.[31] (iii) Based on additional considerations about g value anisotropy, it is concluded that the Si_2 defect is the favored candidate for E'_δ, herewith ignoring the yet solid countering experimental result on equivalent Si sites participating in $a_{\rm iso}$ provided by Buscarino *et al.*[17] (see below).

Buscarino *et al.*[17] were first to properly detect the E'_δ hf structure in the first-harmonic ESR detection mode using RT *X*-band spectrometry. The maximum E'_δ density of $\approx 2 \times 10^{16}$ cm^{-3} was reported for an a-SiO_2 type-I sample Pursil 453, ^{60}Co γ irradiated at RT to a dose of 1000 kGy, subsequently annealed isochronally (~25 min) up to 580 K. Saturation in E'_δ production is observed for doses above ~1000 kGy. The inferred value $(1-\eta)^n R_{\rm hf} \approx 0.16$ was concluded to be compatible with Si_4 and Si_5 configurations, while the O monovacancy dimer model was ruled out. Yet, their observations appear hampered by co-existing other types of interfering signals from centers such as E'_γ, E'_α, $[AlO_4]^0$, and E'_{74} (ascribed to the $O_2H{\equiv}Si^\bullet$ variant[31,44,45] of E'_γ, showing a 74-G split doublet), so more experimental substantiation may be welcome. Following the defect density dependence on $T_{\rm an}$,

a hole transfer from the $[AlO_4]^0$ centers to the precursors of E'_γ and E'_δ centers can occur above 500 K.

III. EXPERIMENTAL DETAILS

A. Sample preparation

The samples investigated, except one, are commercial low OH content fused quartzes or silica: PH370,[46] KI,[47] Infrasil 301,[48] KUVI,[47] Suprasil 300,[48] and Suprasil 311.[48] Only in the first three glasses did we succeed to activate E'_δ signals. According to the supplier, the sample KI has total metallic impurity content (including Al) <15 ppm (by weight) and OH content $\leqslant$0.2 ppm; the KUVI one is specified as metallic impurity content $\leqslant$0.6 ppm, [OH] $\leqslant$0.1 ppm, and [Cl] $\leqslant$0.2 ppm. Sample PH 370 is a low alkaline content fused quartz that came from the manufacturer in the shape of tubes of ~10 mm diameter with ~3.5-mm-thick walls; the other glasses came in the form of slabs 1.8- to 6.6- mm thick. The Suprasil 300 sample contains $\leqslant$1 ppm OH, $\leqslant$0.05 of Na, and $\leqslant$0.05 ppm of Al, while the Suprasil 311 is specified as [OH] $\approx$200 ppm, [Al] $\leqslant$0.01, [Na] $\leqslant$0.01, and [Cl] = 1500 ppm. The types KUVI, Supracil 300 and 311 are synthetic fused silica. The fused quartz Infrasil 301 is detailed as [OH] $\leqslant$ 8 ppm, [Na] = 1 ppm, and [Al] = 20 ppm. Since the sample volume that can be introduced into the ESR cavity is limited, the glasses were cut into thin slices of size $\approx 0.1 \times 2 \times 10$ mm^3 for use in combination with vacuum ultraviolet (VUV) treatments and bars of $\approx 2 \times 2 \times 10$ mm^3 used for UV and γ-irradiation treatments.

After cutting and before applying any other treatment, the silica pieces were etched in aqueous HF (5% HF in H_2O, by volume) to remove cutting damage. In some cases, the etching was also used to thin down slices to desired thicknesses. To ESR activate defects, different samples have been subjected to three types of irradiations: Room ambient VUV (10-eV photons, flux ~10^{15} cm^{-2} s^{-1}) and UV (1.2–6.8-eV range) irradiation was applied using MgF_2-windowed Kr discharge and 150-W Xe arc lamps, respectively. As the penetration depth of VUV photons in a-SiO_2 is ~10 nm,[49,50] the effective sample area is enhanced by stacking thin slices irradiated on both sides. The ^{60}Co γ irradiation was performed at 30 ± 5 °C in dry air at a rate of 40 kGy/h to doses between 20 and 1200 kGy, most samples being irradiated up to 20, 80, 200, 500 kGy, labeled as $R1$, $R2$, $R3$, and $R4$, respectively. Before γ irradiation, part of the KI, KUVI, and Infrasil 301 samples were annealed in vacuum ($<5 \times 10^{-6}$ Torr) at 1175 °C for ~170 min, with the aim to desorb hydrogen (OH groups) from the oxide. Some of the irradiated samples have been selectively treated at desired temperatures in the range 50−346 °C, either in room ambient or Ar, typically for ~8 min.

B. ESR spectroscopy

ESR spectra were taken at three different microwave frequencies, i.e., X (~9.0 GHz), K (~20.5 GHz) and Q band (~34.0 GHz), operated in the T range 4.2–300 K using a Q-band commercial Bruker EMX and locally constructed K-band spectrometer, the latter providing the best sensitivity at low T. Depending on the observational T, X-band observations were made either using a Jeol JES-FA 100 spectrometer (RT investigations) or a locally designed one optimized for low T (liquid He) measurements. All four spectrometers were driven in the adiabatic mode. Routinely, conventional cw low power first derivative-absorption (dP_μ/dB, P_μ being the applied microwave power) spectra were detected through applying sinusoidal modulation (~100 kHz; amplitude $B_m \gtrsim 0.08$ G) of the externally applied static magnetic field $\boldsymbol{B}$. These were complemented with saturation spectroscopy—high-power second-harmonic dispersion mode—measurements (see, e.g., Ref. 30) to disentangle overlapping signals and probe signal line shape.

While generally beneficial for signal sensitivity (Boltzmann factor, noise level, etc.), low-T measurements often suffer from enhanced signal saturation (distortion) effects with decreasing entropy, which requests appropriate reduction of the incident P_μ, at times beyond spectrometer capabilities. This appeared to be a burden for the Q-band spectrometer where, for signals such as E'_δ, E'_α, and E'_γ, the operational P_μ could not be sufficiently reduced to take the signal intensity dependence on P_μ down to the linear range, not even at room temperature (RT) (although it may approach close enough not to induce signal shape distortion, but only intensity modification), so extreme caution is needed in extracting absolute E' densities from those measurements.

Since most of the observed (central) signals are powder patterns, their width is changing with microwave frequency, so the value of B_m was adapted for each individual case to such levels causing no visible signal distortion. For the broader hf structure signals, we used larger B_m values of $\approx$1 G. The signal-to-noise ratio was improved by appropriate signal averaging, depending on the signal strength, even up to 10 000 scans for a single spectrum of the hf structure.

Defect densities were determined through double numerical integration of the detected dP_μ/dB signals using a comounted pointlike reference sample. Depending on spectral composition and/or the ESR parameter aimed to isolate, this was a Si:P marker[51] ($S = 1/2$, $g = 1.998\,69 \pm 0.000\,02$ at 4.2 K), a Li:F marker[52] ($S = 1/2$, $g = 2.002\,29 \pm 0.000\,02$), or DPPH[53] ($S = 1/2$, $g = 2.003\,57 \pm 0.000\,05$ at RT), all three also serving as g markers (attained accuracy $\pm 5 \times 10^{-5}$).

Two simulation codes were used for ESR spectra analysis: Bruker Simfonia (based on perturbation theory, with manual parameter optimization) for E'-type centers in general, and a code based on exact matrix diagonalization (EPR-NMR; courtesy of J. A. Weil) for Al E' centers and the E'_γ and E'_α anisotropic hf structure.

IV. RESULTS AND INTERPRETATION

Here we expand the standard cw absorption ESR research on the E'_δ signal in silica to multifrequency observations at different temperatures to obtain an extended and detailed set of data on the E'_δ center, in particular its hf structure. The a-SiO_2 samples have been subjected to different treatments in an attempt to maximize the intensity of E'_δ defects, both in absolute values as well as relative to the copresent types of other signals.

A. E'-type defects

As to VUV irradiation, E'_δ defects could be generated only in three of the studied silica glasses: PH 370, Infrasil 301, and KI, henceforth referred to as the E'_δ *glasses*. In fact, we did not

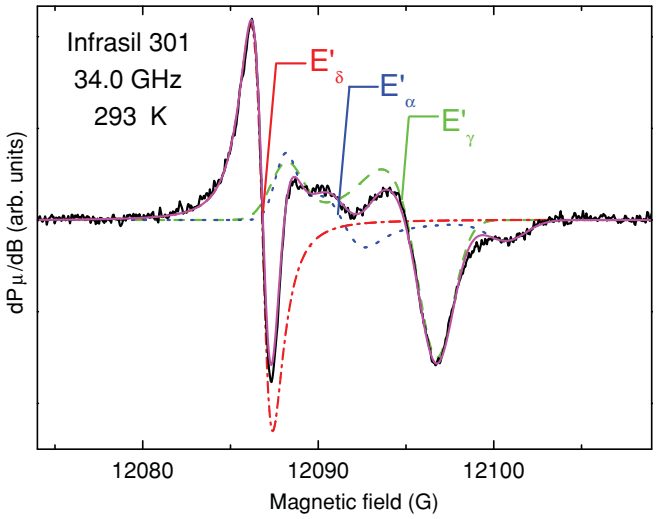

FIG. 2. (Color online) Q-band low power first-harmonic spectrum (central Zeeman part; full curve) of the E' centers measured at RT on Infrasil 301 VUV irradiated for 14 h on each side, using $P_\mu = 1.6 \times 10^{-7}$ W and $B_m = 0.4$ G. The superimposed continuous curve represents the optimized fitting result obtained as a weighed sum of the three constituent signals of which the Gaussian powder pattern fittings, i.e., E'_δ (dot-dashed curve), E'_α (dotted curve), and E'_γ (dashed curve), using the parameters listed in Table I, are also shown.

manage to activate E'_δ centers in KUVI samples with any of the performed treatments (not even after VUV or γ irradiation combined with post-irradiation thermal treatments), unlike previous reports:[54] There, better results were obtained for KUVI than for KI glasses.[55]

Shown in Fig. 2 is a typical RT Q-band spectrum of the near $g \sim 2$ region measured on Infrasil 301 thin slices subjected to VUV irradiation at both sides for 14 h. The spectrum represents a superposition of three signals arising from point defects all considered intrinsic to a-SiO_2 and member of the E'-defect family: E'_α, E'_γ, and the defect of interest, E'_δ. Common for all defects of this group is a principal g value $g_1 \approx 2.0018$ and the fact they all appear associated with an O vacancy in a-SiO_2.

The favored model, underpinned by theory, pictures E'_1 as a positively charged (+1) $O_3{\equiv}Si^\bullet \cdots {}^+Si{\equiv}O_3$ unit[34,41,56] at the site of an O vacancy, that is, composed of an sp^3 hybridized Si dangling bond ($\equiv Si^\bullet$) and a positively charged Si atom backpuckered through its basal oxygen plane towards a lattice O atom that effectively takes threefold coordination. Based on observed ESR parameters,[7] the E'_γ center is considered the closest analog[57] to the basic E'_1 center in α-quartz. Thus the singly positively charged E'_1 crystalline model has been tacitly carried over to the case of E'_γ in amorphous SiO_2, the transference of which appeared well supported by the various results obtained from ESR on a-SiO_2 in combination with electrical charging procedures.[58–60] Yet, in facing experimental facts, it should be cautiously added that the positive charge state of the E'_1 (E'_γ) defect, as laid down in the model for the α-quartz, has so far not been established by *direct* experimental evidence. The complete model is still under dispute.[61] While related to the same generic entity, the overall defect models in α-quartz and a-SiO_2 need not necessarily be the same. In fact, in thermally grown a-SiO_2 on Si, strong evidence has been provided[62] for the E'_γ simply to concern the neutral $O_3{\equiv}Si^\bullet$ unit, i.e., the generic entity of the E' group of defects.

An ^{29}Si hf structure of the E'_γ center in γ-irradiated a-SiO_2 was first observed by Griscom *et al.*[7] revealing a doublet with splitting of $a_{iso} = 420 \pm 3$ G (in unstrained SiO_2), close to the value $a_{iso} = 410$ G reported[63] for E'_1, pointing to a resemblance of E'_γ to the E'_1 defect in α-quartz. The authors also report an anisotropic[7] contribution $a_{aniso} \approx 22$ G to the hf splitting constant.

Griscom[64] first observed the E'_α signal in high-purity a-SiO_2 x-ray irradiated at 77 K, showing $g_1 = 2.0017$, $g_2 = 2.0013$, and $g_3 = 1.9998$ and an associated ^{29}Si hf doublet of 420-G splitting, the same as for E'_γ. The asymmetry of the g matrix was supposed to arise from a Si dangling bond that has in a second-neighbor position an oxygen in a peroxylike linkage, an atom that is displaced from its normal position as a result of irradiation. However, a more recent report[65] revealed that the strong hf structure corresponding to E'_α is in fact a 490-G split doublet—not 420 G—with a g matrix similar to that reported here (see Table I); The successful discrimination compared to initial reports[15,64] may have arisen from different defect activation treatments. The latest model[65] pictures E'_α as a hole trapped at an O vacancy with the unpaired sp^3 Si orbital pointing away from the vacancy in a backprojected configuration and interacting with one more oxygen atom of the a-SiO_2 matrix.[65–67]

As can be seen, e.g., from the Q-band spectrum shown in Fig. 2 observed on Infrasil 301 subjected to VUV irradiation

TABLE I. Inferred Q-band ESR parameters using Gaussian convolution line shapes of width ΔB_{ppi} along the respective g_i axes from optimized spectral simulations of the E'-type centers encountered in all three E'_δ glasses, either VUV or ^{60}Co γ irradiated. A mild annealing step (326−346 °C) was applied to the γ-irradiated samples to maximize the E'_δ defect signal. The two different kinds of irradiation seem to introduce only slight variations in the simulation parameters.

Defect	g_1	g_2	g_3	ΔB_{pp1} (G)	ΔB_{pp2} (G)	ΔB_{pp3} (G)	Irradiation applied
E'_α	2.0017	2.0012	1.9996	1.2	2	2.2	VUV
	2.0018	2.0009	1.9997	0.6	1.8	2.1	γ
E'_γ	2.0017	2.0005	2.0003	1.8	2.7	1.8	VUV
	2.0018	2.0005	2.0003	0.57	1.37	1.1	γ
E'_δ	2.0018	2.0020	2.0020	0.9	1.4	1.25	VUV
	2.0019	2.0020	2.0020	3	0.6	0.8	γ

TABLE II. Inferred densities of observed E'-type centers in those vitreous silica samples in which the E'_δ signal could be activated by irradiation, together with some sample treatment specifications. As VUV is penetrating only a surface layer (∼10 nm) in contrast with γ irradiation, the defect densities are specified in units of cm^{-2} or cm^{-3}, respectively. Where not specified, relative errors on the inferred densities are estimated at ⩽6%. For the VUV irradiation, the indicated exposure time is per sample side.

Sample designation	Irradiation treatment	Additional anneal (≈336 °C; air; 8 min)[a]	(E'_δ)	(E'_α)	$[E'_\gamma]$	(Al E')[b,c]
PH 370	VUV (201 h)	−	$(3.5 \pm 1) \times 10^{13}$	$(5.4 \pm 0.5) \times 10^{13}$	$(1.1 \pm 0.1) \times 10^{14}$	NA
	γ (500 kGy)	−	$<1 \times 10^{14}$	2.5×10^{16}	2.6×10^{17}	3.1×10^{15}
		+	9.6×10^{14}	2.9×10^{16}	2.1×10^{17}	NO
Infrasil 301	VUV (77 h)	−	$(7.9 \pm 0.7) \times 10^{12}$	2.6×10^{13}	$(1.9 \pm 0.2) \times 10^{13}$	NA
	γ (500 kGy)	−	$<5 \times 10^{14}$	5.6×10^{16}	5.3×10^{17}	3.0×10^{15}
		+	$<5 \times 10^{14}$	3.3×10^{16}	3.1×10^{17}	NO
KI	VUV (20 h)	−	1.4×10^{13}	7.9×10^{13}	4.0×10^{13}	NA
	γ (200 kGy)	−	$<7 \times 10^{13}$	$<4.7 \times 10^{15}$	2.8×10^{16}	3.0×10^{15}
	γ (200 kGy)	+	$(1.1 \pm 0.1) \times 10^{16}$	$(2.9 \pm 0.2) \times 10^{16}$	$(4.0 \pm 0.2) \times 10^{16}$	NO
	γ (500 kGy)	−	$<8 \times 10^{14}$	$<9 \times 10^{15}$	4.1×10^{16}	4.7×10^{15}
	γ (500 kGy)	+	1.5×10^{16}	3.4×10^{16}	6.5×10^{16}	NO

[a]-: not applied; +: applied.
[b]Though useful for relative comparison, the specified Al E' densities in absolute terms should be considered rather as indicative, as these are obtained assuming that the Al E' signal exhibits the same saturation properties as the strong E'_γ hf doublet.
[c]NO: not observed; NA: not available

(14 h, both sides), the overlap of the E'_α, E'_δ, and E'_γ signals makes disentanglement tedious, with consequential impact on the precision attained of the ESR parameters inferred through spectra simulation using, e.g., the Simfonia software.

Simulations of the central part of the observed E' defect spectra has been carried out for all three types of E'_δ silica, and for both VUV and γ-irradiation treatments, using Gaussian convolution line shapes. The inferred principal axes g_i values and applied broadenings ΔB_{ppi} ($i = 1,2,3$) are listed in Table I, where, consistently, the g-value fitting parameters per kind of defect agree within experimental error for the two irradiation treatments. Yet, to be noted here is that compared to γ rays, VUV irradiation generally leads systematically to a larger width of the Gaussian broadening functions (except for the g_1 direction of E'_δ). As one possibility, it may be due to the larger local defect density (e.g., dipolar interaction) over the limited VUV penetration depth. As illustrated in Fig. 2, the experimental spectra could be accurately simulated, from where the defect densities listed in Table II are obtained. As to the PH 370 glass provided in the shape of tubes, there was no difference in of E'_δ defect appearances between inner and the outer surface subjected to VUV irradiation.

B. E'_δ optimization

The correct measurement of the E'_δ hf structure intensity using the mandatory first-harmonic detection mode requires, for sensitivity reasons, the utmost optimization of the E'_δ defect density. For this end, in a comparative manner, different irradiation treatments in combination with thermal steps have been explored.

The influence of VUV irradiation time on the induced E'_δ defect density was monitored for the three E'_δ glasses by Q-band measurements taken within maximum a few days after each irradiation step; Fig. 3 shows the evolution for the Infrasil 301 sample. Left in room ambient, neither the E'_δ signals nor those of other E' centers were found to change appreciably over months after irradiation. The E'_δ density in VUV irradiated samples could be somewhat improved by thermal treatment, yet not significantly.

Figure 4 shows some representative 200-G wide Q-band spectra (i.e., excluding the E'_γ and E'_α strong hf structure range) observed after intensive VUV irradiation on the PH370 (≈201 h; bottom curve) and KI (≈77 h; middle curve) glasses. As it offers a generally much enhanced signal-to-noise ratio in the case of highly saturable (low defect density) signals, the second-harmonic saturation detection method is used here to optimally trace and reveal occurring hf structure signals. In the ≈100-G splitting range, two main doublets, of 74- and 120-G splitting, are observed, badly overwhelming the targeted E'_δ hf

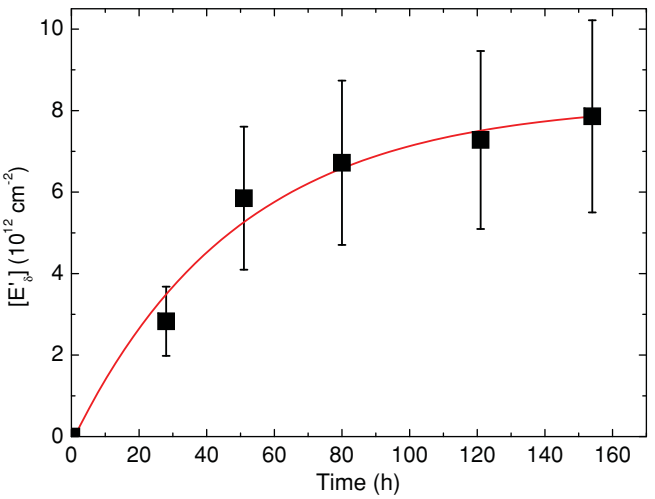

FIG. 3. (Color online) Evolution of E'_δ defect production as a function of the total VUV irradiation time in Infrasil 301 glass. The curve is meant to guide the eye.

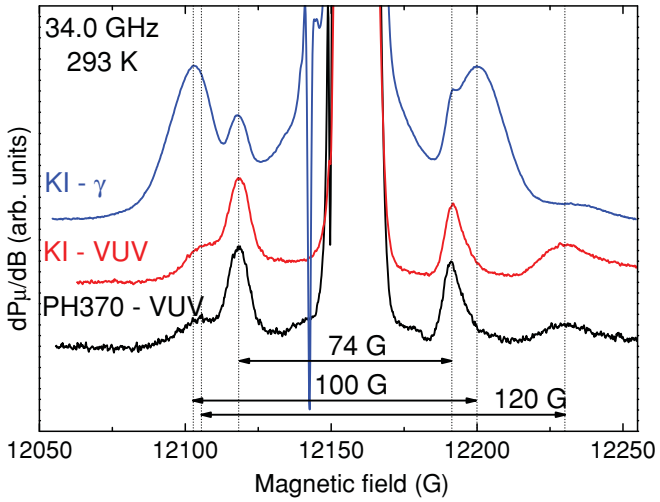

FIG. 4. (Color online) Comparison of representative high power second-harmonic Q-band ESR spectra measured at RT using $P_\mu = 1.6$ mW and $B_m = 0.5-1$ G on two types of silica subjected to γ (and subsequent anneal at 336 °C, 8 min, air) and VUV irradiation. The spectra, normalized to the central E'_γ signal, are enlarged to expose the hf structure in the 'neighborhood' of the central E' main signals (blown up off scale in the center of the spectrum). The 120-G doublet, ascribed to an $O_2H{\equiv}Ge^\bullet$ defect, is quite intense in the VUV-irradiated samples spectra, normalized to the central E'_γ signal, while it appears relatively much reduced in the γ-irradiated sample. The 100-G split E'_δ hf doublet is clearly prominent only in the γ-irradiated sample spectrum. The 74-G split doublet stems from the E'_{74} ($O_2H{\equiv}Si^\bullet$) defect.

structure of interest. The spectra here were normalized to the amplitude of the central E'_γ (absorptionlike) signal.

The 74-G doublet, centered at $g \approx 2.0016$, stems from the E'_{74} defect,[31,68] evidencing the silica to contain OH groups.[44] A doublet of ≈119-G splitting, associated with a defect of axial[69] g symmetry ($g_\perp = 1.999 \pm 0.001$, $g_\parallel = 1.992 \pm 0.001$), was modeled as an irradiation-induced impurity-related defect which involves an electron trapped at a H-compensated Ge impurity in a-SiO_2 ($O_2H{\equiv}Ge^\bullet$). The signals of the VUV-activated 120-G doublet here, measured in the unsaturated first-harmonic mode (not shown), exhibit similar asymmetric shapes as reported before.[69] However, there is no indication of Ge in the supplier's specifications of glass composition.

For the current purpose, the observations such as illustrated in Fig. 4 immediately bear out the inadequacy of the VUV treatment for these kinds of glasses, a situation which cannot be cured, not even by extended VUV irradiation times. Reliable extraction of the E'_δ-associated 100-G hf doublet appears virtually impossible, a situation even far worse for the first-harmonic detection mode method. So, VUV irradiation is concluded to be inadequate for this purpose.

Also attempted was subjecting the E'_δ glasses to UV irradiation, which is supposed to partially bleach the 74-G doublet.[44] While much more deeply penetrating into the sample, unfortunately, UV treatment was found to activate only E'_γ and E'_α defects, in line with previous results.[45,70,71] We found no trace of E'_δ, thus outright disqualifying UV irradiation for the intended purpose.

Separate samples of the three glasses that showed E'_δ signals after VUV treatment were γ irradiated with doses of 20, 80, 200, and 500 kGy: indeed, again an E'_δ signal was found to be generated in all three glasses, albeit small in comparison to E'_γ and E'_α. Noteworthy is that in the other glasses γ irradiated to the highest doses, still no E'_δ signal could be observed. Thus only three types of the investigated glasses appear prone to E'_δ generation, and by both VUV and ^{60}Co γ irradiation. From the four applied γ doses, the 200-kGy one seems best in terms of E'_δ intensity *relative* to the E'_γ and E'_α signals and overall spectral appearance, although 80- and 500-kGy irradiations gave satisfactory results as well. In an attempt to reduce the H-related 74-G doublet also observed after γ irradiation, some samples were vacuum annealed (1175 °C) before γ irradiation, yet without ensuing any noticeable difference. In line with previous work,[17] applying thermal treatment after γ irradiation increases the absolute E'_δ density drastically (orders of magnitude) as well as increasing its density relative to those of the (invariably) copresent E'_γ and E'_α defects. The former effect is demonstrated in Fig. 5 by isochronal annealing (8 min) results of the absolute E'_δ defect density in γ-irradiated (200 kGy) KI silica as a function of T_{an}, indicating that an optimum is reached for $T_{an} \approx 326$ °C, similar to previous results.[17] This establishes the current optimum E'_δ generation method.

In Fig. 4 is shown a Q-band second-harmonic saturation spectrum (top curve) observed on a γ irradiated (200 kGy) KI sample subsequently annealed at ∼336 °C, where now the 100-G E'_δ hf doublet is clearly and intensely revealed, much enhanced (compared to the VUV data) relative to the copresent 74- and 120-G doublets. Pertinently, the applied thermal step also eliminates at once the $S = 1$ triplet state spectrum.[15] It opens the route for proper E'_δ hf structure analysis, i.e., signal disentanglement and correct intensity determination. Here again we should stress the (drastic) influence of post-irradiation annealing, to such extent that in the as-γ-irradiated state, the observed E'_δ signal intensities did not much exceed the VUV results.

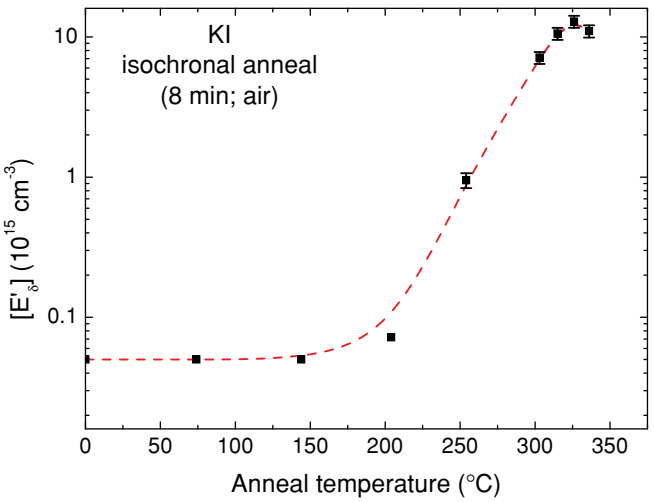

FIG. 5. (Color online) Variation of the E'_δ density for the 200-kGy γ-irradiated KI sample as a function of cumulative 8-min isochronal annealing. The saturating maximum density is obtained for ≈ 326 °C. Densities were determined from first-harmonic Q-band spectra taken at RT. The curve guides the eye.

Over all the E'_δ glasses, we also monitored the strong hf structure splitting of E'_γ and E'_α defects, reported to be $a_{iso} \approx 420$ G,[7,30,72] $a_{aniso} \approx 22$ G, [7] and $a_{iso} \approx 490$ G,[65] respectively. Optimized fitting (EPR-NMR software) of the E'_γ and E'_α hf signals (powder patterns) using Gaussian convoluting line shapes (width $\Delta B_{pp} = 26.5$ and 45 G, respectively) gives the average hf matrix values $a_{iso} = 424 \pm 4$ G, $a_{aniso} = 20 \pm 3$ G and $a_{iso} = 455 \pm 4$ G, $a_{aniso} = 20 \pm 3$ G for the E'_γ and E'_α defect, respectively. The substantial difference of the E'_α a_{iso} value with literature data is likely due to having carried out a fitting involving both a_{iso} and a_{aniso}, in contrast with previous work.[65] For all samples in which E'_δ defects are observed, we find that the E'_γ apparent hf splitting (the distance between the tops of the simulated absorptionlike signals) is in the range 421–424 G, that is, somewhat larger than the average 418-G value.[11] The increased splitting has been ascribed to enhanced local strain in the vicinity of the E'_γ defects.[11] Local strain in the oxide may be beneficial for E'_δ defect generation.

C. Al-related signals

During second-harmonic saturation mode measurements over enhanced magnetic field ranges, we noticed the presence in some samples of a low intensity six-line spectrum which was readily traced back as originating from the Al E' center,[73,74] the six-line structure stemming from the interaction of the unpaired electron with an Al nucleus ($I = 5/2$; $\eta = 99.9\%$). The observed signal is illustrated in Fig. 6, showing a RT Q-band second-harmonic saturation spectrum observed on a γ-irradiated (200 kGy) KI sample. Inferred defect densities

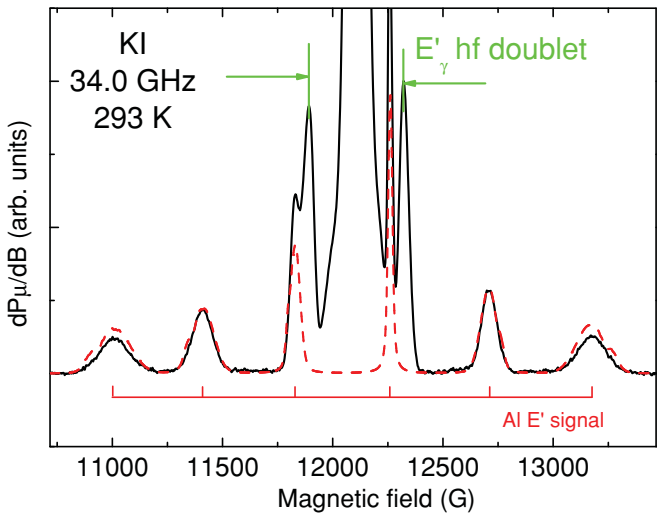

FIG. 6. (Color online) Room-temperature Q-band second-harmonic saturation spectrum (full curve) observed using $P_\mu = 1.6$ mW and $B_m = 1.5$ G on sample KI after 200-kGy γ irradiation in the as-irradiated state, clearly showing the ^{27}Al hf six-line spectrum of the Al E' center. The superimposed dashed curve represents an optimized computer simulation giving $a_{iso} = 416$ G, $a_{aniso} = 16$ G, $g_{iso} = 2.0011$, and $g_{aniso} = 0.0007$ with a Gaussian distribution in a_{iso} of $\Delta a_{iso} = 26$ G, and where a Gaussian convolution function of width $\Delta B_{pp} = 12$ G has been used. For more details, see text. The main 420-G E'_γ hf doublet is also marked. The off scale central part of the spectrum corresponds to the E' main signals.

are listed in Table II. Since the signal eludes standard first-harmonic detection (too weak), these have been determined from the second-harmonic saturation spectra through simulation of the observed spectra (see below) and assuming similar saturation behavior of the Al E' and E'_γ centers: the intensity of the six-line spectrum simulation was compared to that of the 420-G E'_γ doublet detected in the same scan, where the correct E'_γ defect density corresponding to the doublet (4.90% of the central line) was independently obtained from low power first-harmonic spectra by comparison to a comounted marker. Optimized Al E' signal simulation was obtained using the ESR parameters: $a_{iso} = 416$ G, $a_{aniso} = 16$ G, $g_{iso} = 2.0011$, $g_{aniso} = 0.0007$, a Gaussian distribution in a_{iso} of spread $\Delta a_{iso} = 26$ G (standard deviation), and a Gaussian convolution function of width $\Delta B_{pp} = 12$ G. To emulate this distribution on a_{iso} we have calculated spectra for twenty a_{iso} values evenly spread over the whole Gaussian a_{iso} interval, and added the weighed spectra to obtain the simulation shown in Fig. 6. While reliable relatively, the inferred densities in absolute terms should be considered rather as indicative. As is clear from Table II, the Al E' signal is observed, *before annealing*, in γ-irradiated samples, but only in those that also show the E'_δ signal (the E'_δ glasses); annealing at ~326 °C eliminates the Al E signal.

The Al E' center first observed by Brower[73,74] in natural vitreous silica exposed to ionizing irradiation was attributed to an electron captured on an ^{27}Al atom in a Si-substitutional position bonded to three oxygen atoms in the a-SiO_2 matrix ($[A1O_{3/2}]^-$ defect). Pertinently, the center was found to need a charge compensator to remain paramagnetic (ESR-active) above 57 °C; it stays paramagnetic up to 277 °C if stabilized by alkali ions and up to 377 °C if hydrogen is involved, otherwise it turns to its neutral diamagnetic $Al{\equiv}O_3$ ($AlO^0_{3/2}$) state. As analyzed in detail,[73,74] the hf coupling tensor is influenced by the compensating agent. In the current case, the compensating agent[74] is likely Na^+, as suggested by the simulation parameters and the observation that the signal disappears after annealing at 326 °C in all the E'_δ samples.

As illustrated in Fig. 7 showing a first-harmonic RT X-band spectrum taken on γ-irradiated (200 kGy) and subsequently annealed (~336 °C) KI silica, there is a prominent broad signal overlapping the E'-defect range. The superimposed powder pattern simulation is obtained using Lorentzian broadening functions of width $\Delta B_{pp1} = 6.0$ G, $\Delta B_{pp2} = 6.5$ G, and $\Delta B_{pp3} = 10.5$ G along the principal (g_1, g_2, g_3) axes, respectively, and using the g values reported in the literature for the neutral $[AlO_4]^0$ center in both crystalline[75,76] and vitreous[77] SiO_2, that is, $g_1 = 2.060$, $g_2 = 2.008\,54$, $g_3 = 2.001\,95$, and[76] $a_{iso}(^{27}Al) = 8.4$ G. The satisfactory fitting convincingly assigns this signal[17] to an Al atom substituting for a four-coordinated Si with an unpaired electron in a nonbonding $2p$ oxygen orbital of a bridging oxygen atom.[76] This signal, extending over an ~100-G wide range at X band (cf. Fig. 7) comes as a background on top of the E' spectra: it poses no substantial problem for small-width small-B_m sweeps probing the central E' center lines (see, e.g., Fig. 2), yet for broader sweeps probing the E' hf structure using high(er) B_m, it does interfere. So, its presence has to be additionally taken into account for correct spectroscopic assessment of the E'_δ (100-G doublet) hf structure, cf. Fig. 7, where the high-field 100-G doublet signal is marked by arrow 2.

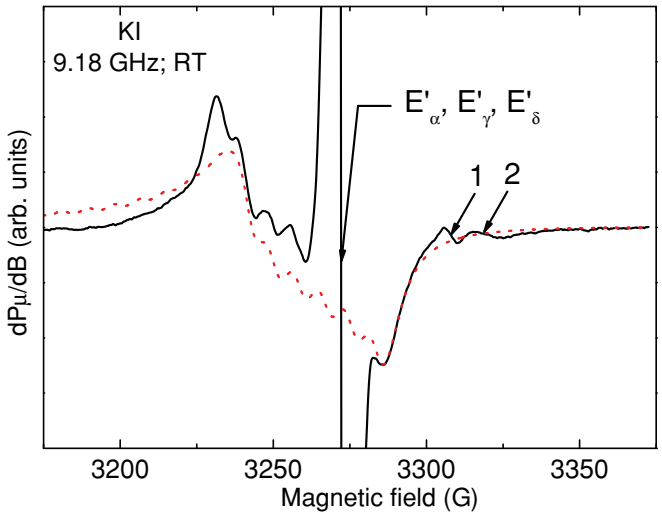

FIG. 7. (Color online) First-harmonic X-band RT spectrum (full curve) observed using $P_\mu = 0.01$ mW and $B_m = 2.5$ G on sample KI γ irradiated to a dose of 200 kGy and subsequently annealed at 326 °C (8 min). In addition to the summed central main Zeeman E'_α, E'_δ, and E'_γ signals (off scale), the spectrum shows the $[AlO_4]^0$ signal. The high-field components of the 74- and 100-G hf doublets are indicated by arrows (1) and (2), respectively, the low-field components being masked by the overlapping $[AlO_4]^0$ signal. The dotted curve represents a powder pattern simulation obtained using $g_1 = 2.060$, $g_2 = 2.008\,54$, and $g_3 = 2.001\,95$, Lorentzian broadening functions of width $\Delta B_{pp1} = 6.0$ G, $\Delta B_{pp2} = 6.5$ G, and $\Delta B_{pp3} = 10.5$ G along the principal g axes, respectively, and $a_{iso}(^{27}Al) = 8.4$ G. The figure clearly illustrates that it is the Lorentzian tail of the $[AlO_4]^0$ signal which predominantly obscures the indicated hf structure, not the Gaussian tail of the central E' signals.

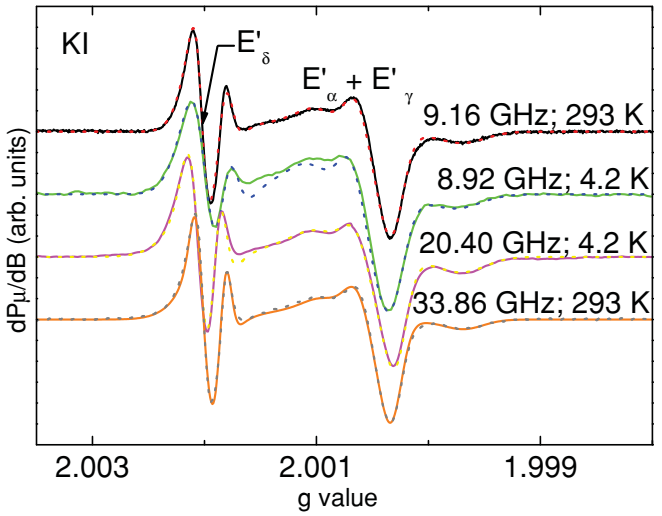

FIG. 8. (Color online) First-harmonic low power ($P_\mu \leqslant 1.6 \times 10^{-7}$ W and $B_m < 0.25$ G) spectra of the central E' signals measured on γ-irradiated (200 kGy) and subsequently annealed (336−346 °C; air) KI samples at indicated microwave frequencies and temperatures. Superimposed on each spectrum (dotted curve) is the weighed sum of separately optimized simulations of the constituent E'_α, E'_δ, and E'_γ signals using the g values listed in Table I, and for the Q-band spectra, the listed widths ΔB_{ppi} of the applied Gaussian broadening functions; the latter were somewhat adapted for X- and K-band signals.

D. E'_δ spectrum and line shape

As concluded previously, over all the a-SiO_2 samples studied and treatments applied here, the γ-irradiated (200 kGy) and subsequently annealed (315−336 °C) KI sample turns out as optimal for the study of the E'_δ signal and corresponding hf structure. Figure 8 shows a selection of low power first-harmonic ESR spectra of the E' main signals measured on such KI silica in four spectrometers at 4.2 K or RT, as indicated. Because of the limited potential in lowering of the operational P_μ of the Q-band spectrometer, it is felt that, even for the lowest P_μ realized, the recording of the central E' signals may still be at the edge of being "saturation free", which would cast doubt on the correct extraction of signal intensities and the absolute defect densities (e.g., Fig. 8, bottom spectrum): So, while the spectral shape parameters obtained from simulation are considered reliable, only X- and K-band data are used for density and R_{hf} determination. The dotted curves in Fig. 8 represent optimized spectra simulations, each obtained as a weighed sum of the individual E'_δ, E'_α, and E'_γ signal simulations using the parameters listed in Table I and Gaussian convoluting line shapes. From X- and K-band simulations like these we obtained the individual E'_δ, E'_α, and E'_γ defect densities (cf. Table II).

For the splitting of the E'_δ hf doublet we measure 100 ± 1 G for all three microwave frequencies, independent of T in the interval 4.2–300 K. Figure 9 shows representative high P_μ second-harmonic phase quadrature spectra observed at various microwave frequencies and temperatures on the annealed (336−346 °C)γ-irradiated KI silica, focused on the E'_δ hf structure spectral region. In this detection mode the hf signals appear as closely resembling the direct absorption shapes, and because of the offered enhanced sensitivity, these spectra were taken to analyze, in a comparative manner, the E'_δ hf signal shape over various observational T's and microwave frequencies. From spectral simulations, optimized at the less perturbed high-field signals (cf. dotted curves in Fig. 9), it is inferred that both the 74- and 100-G doublets peak shape is closely Gaussian with $\Delta B_{pp} = 3.7 \pm 0.5$ G and 15 ± 0.5 G, respectively, independent of observational f_μ and T within experimental error; there may be present, though, a weak dependence (broadening) of the 74-G doublet signal width on f_μ. The constant broadening likely results from strain-induced spread in (principal) hf matrix constants (a_{iso}, a_{aniso}). This assembled information is considered essential for the final step in assessment, that is, correct interpretation of the cautiously measured first-harmonic E'_δ hf structure.

Since the E'_δ center is considered as part of the same defect family as E'_γ (and perhaps E'_α) for which we need anisotropic hf matrices to correctly simulate the corresponding doublets, we also tried to fit the 74- and 100-G doublets using appropriate anisotropic hf matrices. Yet, due to the rather small hf splitting in combination with the limited g anisotropy for both doublets, the added hf anisotropy barely affects the doublet shapes. Therefore, within the view of limiting the number of variables for the same result, we simulated the doublets as being isotropic Gaussians, but still recall that an anisotropic line shape may apply as well.

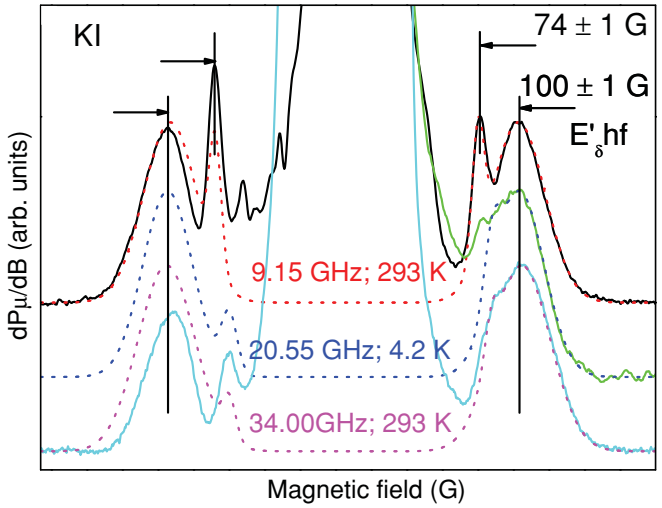

FIG. 9. (Color online) Second derivative phase quadrature saturation spectra ($P_\mu \leqslant 1.6$ mW, $\Delta B_{pp} \leqslant 1.5$ G) obtained on the same KI samples as dealt with in Fig. 8. The superimposed dotted curves each represent the weighted sum of the simulation of two isotropic doublets using Gaussian shapes, corresponding to the 74-G (E'_{74}) and E'_δ ^{29}Si 100-G split hf doublets, as indicated. The extracted simulation parameters were used for disentangling the corresponding direct detection (first harmonic) mode spectra shown in Fig. 10. In the K-band spectrum (middle curve) the left side is overwhelmed by the $[AlO_4]^0$ absorption signal (off scale at the low magnetic field side of the spectrum).

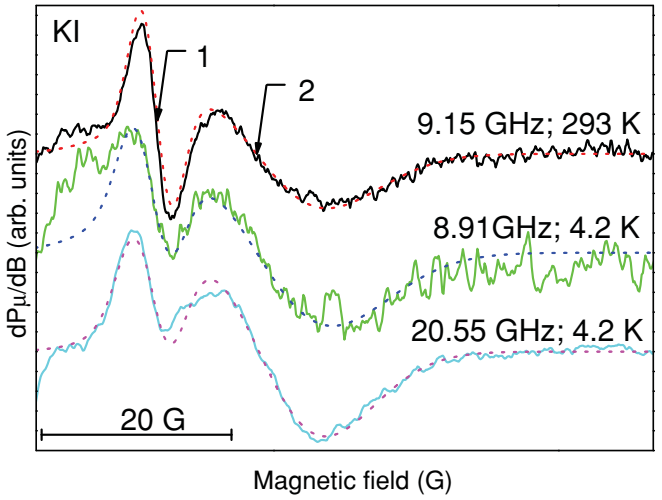

FIG. 10. (Color online) First-harmonic low power mode ESR spectra measured, using $B_m < 1.3$ G, at various microwave frequencies and two temperatures on the sample the ^{60}Co γ-irradiated KI samples addressed in Figs. 8 and 9. The spectral window is focused on the high-field signals of the 74-G (1) and E'_δ 100-G hf (2) doublets, as indicated. The field range covered here corresponds to the $g \approx 1.95-1.98$ range for X-band ESR. The observed curves have been corrected for an underlying Lorentzian background shape pertaining to the overlapping $[AlO_4]^0$ signal. Making use of the previously derived spectral information from measurements such as those shown in Figs. 7 and 9, the dotted curves represent optimized simulations, where a small f_μ-dependent broadening of the E'_{74} hf doublet line has been incorporated. In combination with the analysis of the central E'_δ signal, the R_{hf} ratio inference was based on these simulations, leading to an average value $R_{hf,av} = (20.3 \pm 1.9)\%$.

Unlike X- and Q-band RT observations, in the K-band low-T (4.2 K) saturation spectra we also observe the $[AlO_4]^0$ absorption signal, probably due to a favorable choice of parameter settings (see, e.g., Fig. 9). That is why for the K-band spectra we restricted the simulations to the high-field peaks (cf. Fig. 9).

Since the E' central signals and the 100-G doublet hf peaks show distinct differences in width, amplitudes, and saturation levels, we chose to adapt part of the measurement parameters, like B_m and P_μ, so as to individually optimize the signal-to-noise ratio for each type of signal studied, yet without distorting it. For this reason, measuring the two groups of signals in the same scan proved not optimal, so we measured them separately but we carefully compensated for the different parameter settings used when calculating the corresponding intensities and densities.

As a main focal point, Fig. 10 shows zoomed in low P_μ and B_m first-harmonic spectra observed at various f_μ's and T's of the high-field component of the E'_δ hf doublet, with, on top, the analogous 74-G doublet component (marked 2 and 1, respectively). The signals have been corrected for an underlying Lorentzian background pertaining to $[AlO_4]^0$ centers. Indeed, as evident from Fig. 7, the high-field E'_δ hf peak is mainly perturbed by this $[AlO_4]^0$ signal shape and not by the tail of the central E' signals. The dotted curves in Fig. 10 represent optimized simulations for which the previously inferred information (line shape, broadening) from the corresponding saturation spectra has been consistently used. Finally, from this detailed hf structure analysis combined with the (previously) inferred intensities of the central E'_δ ESR signal, we obtain over the analysis of various spectra for R_{hf} the values $(19.7 \pm 2.5)\%$ at 4.2 K and $(20.3 \pm 2.0)\%$ at RT from X-band measurements, and $(20.9 \pm 1.3)\%$ for the K-band 4.2-K data, where the error bars represent standard deviation. Reassuringly coinciding within experimental error, the data directly and importantly show R_{hf} to be *T-independent* over the range 4.2–295 K as is the case for the g matrix as well. It indicates there would be no dynamic averaging effect of the unpaired electron involved. Averaging over all measured data points obtained from measurements at different frequencies and temperatures we obtain, as a global average, $R_{hf,av} = (20.3 \pm 1.9)\%$.

V. ANALYSIS AND DISCUSSION

A. E'_δ occurrence and stability

Over all the vitreous silica glasses studied, and the three types of irradiations applied, we found that the E'_δ signal could only be produced in three kinds of silica: PH370, Infrasil 301, and KI (cf. Table II), and this only, yet always also, by two types of damaging: VUV and ^{60}Co γ rays. But with the E'_δ signal barely detectable in the as-irradiated state, the latter method requires an extra post-irradiation short anneal (≈326 °C; 8 min) to fully turn on the E'_δ defect signal (∼10–100-fold increase). No such anneal is required after VUV irradiation. No E'_δ could be produced by UV photons, in agreement with previous work;[45,78] only E'_α and E'_γ signals were observed.

We should underline the fact that the VUV and ^{60}Co γ irradiations come as a match for each other in terms of effective E'_δ production. Given the distinct disparity regarding the energetic quantum involved (10 eV vs ~1.17- to 1.33-MeV photons), this clearly bears out the importance of the glass nature for E'_δ occurrence in that it must meet some precursor requirements such as, likely for the current case, O deficiency and possibly, the presence of charge compensating units.

Furthermore, comparison of UV with VUV and γ irradiation results suggests that E'_δ signal activation starts from preexisting sites: indeed, the observation that the E'_δ signal appears after irradiation with $h\nu > E_{g,\mathrm{SiO_2}}$ (the SiO_2 band gap; over band gap excitation) indicates ESR defect activation as a result of ionization rather than the displacement process. Also, as to the applied UV doses, the two-photon process[79] appears insufficient for the E'_δ activation to a detectable level, unlike the E'_γ and E'_α cases. We further notice that, compared to γ damaging, VUV irradiation appears almost exhaustively efficient on this matter, as an additional thermal step only slightly increases the E'_δ signal. In one view, if charge compensators are involved,[80] it might indicate that an intense fluence of VUV photons over a limited volume may enhance compensator migration at RT.

As to γ irradiation, about the maximum volumetric E'_δ density of $\approx 1.1 \times 10^{16}$ cm^{-3} is obtained for KI silica subjected to 200-kGy ^{60}Co γ rays and subsequent thermal treatment at 336 °C. For comparison, VUV irradiation for 20 h (each side) of the same KI silica results in an areal E'_δ density $\approx 1.4 \times 10^{13}$ cm^{-2} (determined from the main central ESR line) located in the thin surface layer it penetrates. If assuming a mean VUV penetration depth[49,50] of ≈10 nm, this would translate to a volume density of $\approx 1.4 \times 10^{19}$ cm^{-3}—much larger than the above volumetric density obtained by ^{60}Co γ irradiation. However, this value is likely overestimated: If assuming, as likely, that the over band-gap *e-h* pair production is essential in ESR-activating E'_δ defects, the much deeper in diffusing *e-h* pairs (orders of magnitude)[81] will result, more likely, in a local E'_δ density in the range $(1-10) \times 10^{16}$ cm^{-3}, compatible with the ^{60}Co γ-irradiation result. Yet, it cannot be excluded that SiO_2 layers closer to the surface are more prone to E'_δ production as, e.g., reported before for BOX.[18] It may be the case for the E'_δ glasses (cf. Table II).

Left in room ambient after production by irradiation, the E'_δ signal was found to bleach in time, though on a larger time scale than reported before. For VUV-activated E'_δ centers, the decay time is $\gtrsim 1$ yr, while $\gtrsim \frac{1}{2}$ yr for γ-ray treatments. This contrasts with the behavior reported for BOX samples, where almost total bleaching of the E'_δ signal is observed about days after activation with positive biased corona/VUV,[20] or conventional electrode positive bias/VUV photoinjection,[25] and weeks in the case of positive dc glow discharge irradiation.[25] Interestingly, regarding this E'_δ signal decay, the former ESR work has suggested direct evidence for an increase of the E'_γ signal at the expense of E'_δ centers due to direct defect-defect hole transfer.[20]

B. E'_δ: hf structure intensity

As firmly evidenced in previous ESR works,[15,17] the observed 100-G doublet constitutes the principal hf structure associated with the E'_δ center, showing close correlation, both qualitatively and quantitatively, with the central E'_δ Zeeman signal. Stepping from the intrinsic nature of the E'_δ center (no direct involvement of an impurity in the defect kernel) its revealed hf structure is based on the nonzero nuclear spin ($I \neq 0$) isotope composition of ordinary SiO_2, logically ascribed to interaction of the unpaired electron with the ^{29}Si ($I = 1/2; \eta = 4.67\%$) isotopes. On the grounds of ESR feasibility considerations, interaction with ^{17}O ($I = 5/2; \eta = 0.034\%$) is excluded as an alternative.

As outlined, a decisive key factor in steering reliable atomic defect modeling is the number n of (largely) equivalent Si sites involved in the hf interaction, that is, over which the unpaired electron wave function is mainly delocalized. This must be obtained from correct determination of the ratio $R_{\mathrm{hf}}(\eta,n)$ which for small η values is given to good approximation by the expression

$$R_{\mathrm{hf}} = \frac{I_{\mathrm{hf}}}{I_c} = \frac{\eta n(1-\eta)^{n-1}}{(1-\eta)^n} = \frac{\eta n}{1-\eta}, \qquad (1)$$

where the simultaneous occurrence of two or more $I \neq 0$ isotopes in a shell has been neglected (for Si, the maximum error is <0.002 for $n < 6$). The expected values for different Si shells ($n = 1-6$) are listed in Table III, where P_{29} and P_{28} represent the probability for finding one and zero ^{29}Si isotopes in a shell, respectively.

Comparison to Table III of the experimentally inferred value $R_{\mathrm{hf,av}} = (20.3 \pm 1.9)\%$, averaged over all T's and f_μ's, clearly shows that the $n = 2$ case (Si_2 dimer model) invariably promoted by theory is to be ruled out definitively, in agreement with previous results.[17] In passing, to remunerate first assignment,[15] there should therefore be an overturn in labeling, that is, the Si_2 (charged Si dimer) defect calculated by theory[12,33,36,39,41] should no longer be labeled as E'_δ, the label first given to the observed ESR spectrum. In fact, the comparison shows that the experimental R_{hf} value falls between $n = 4$ and $n = 5$, closest to the former, concluding that the four-Si case would seem straightforward. Yet, some caution may be needful. To conform to scientific rigor, we here should refer to the experimental determination of R_{hf} pertaining to other point defects involving unpaired sp^3 Si hybrids in Si/SiO_2 entities. Indeed, previous works have reported on measured R_{hf} values generally somewhat smaller than expected, where the loss in hf intensity was attributed to *broadened portions* of the ^{29}Si spectrum lost in the noise[82] as

TABLE III. Values of R_{hf}, the ratio of the hf structure intensity to that of the main resonance line, calculated using Eq. (1). Here, P_{29} represents the probability of only one ^{29}Si ($\eta = 4.67\%$) isotope occurring over the n possible sites, while P_{28} is the probability for none.

n	P_{29}	P_{28}	R_{hf}
1	0.047	0.953	0.049
2	0.089	0.908	0.098
3	0.127	0.866	0.147
4	0.162	0.825	0.196
5	0.193	0.786	0.245
6	0.221	0.749	0.294

a result of varying local strain over the defect sites.[83] On this account, we should not exclude $n = 5$ as a valid option.

But, looking deeper, based on the current strict result, neither of these can be retained on theoretical grounds, basically because, as unanimously calculated by many works,[12,32,33,37] the spin density of the unpaired Si electron asymmetrizes for whatever cluster model, in the sense that it gets localized to a large extent in an elongated bond between two adjacent Si atoms (Si_4), or primarily on the central atom (Si_5). So these models would, like the Si_2 one, correspond to the $n \leqslant 2$ situation as well. This leaves us with an uncomfortable hiat: there appears so far no acceptable atomic model for E'_δ at hand. Hinging on theory, it means that our current perception of the E'_δ center needs revolutionizing, as will be elaborated upon below.

C. E'_δ correlation with Al-related defects

A noteworthy observation is that, as to the ^{60}Co γ-irradiation damaging, we could observe (generate) an E'_δ signal (albeit after annealing) only in those studied vitreous silica types also showing the Al E' center (perhaps compensated by the Na^+ ion in its vicinity) in the nonannealed as-irradiated state; as is seen from Table II, all three E'_δ-silica exhibit an Al E' density in the range $(3-5) \times 10^{15}$ cm^{-3}. As is also evident from Table II, no Al E' signal could be detected after VUV irradiation, which, however, does turn on the E'_δ ESR signal. This is ascribed to the limited penetration depth of the VUV irradiation in SiO_2, failing to establish an ESR-detectable sufficient overall number of Al E' centers within one ESR sample in the cavity. We further notice that there seems to be no correlation between the occurrence of E'_γ and Al E'.

So, the revealed systematic co-presence of Al impurities, here exposed in the form of Al E' centers, might suggest some determinative influence on E'_δ generation. Obviously, within the current admitted understanding of both types of defects, the process cannot concern direct charge transfer between the centers, i.e., electron transfer from the neutral E'_δ precursor to the negatively charged Al E' center. Yet, dealing with charged defects, as admitted, the negatively charged Al E' center (without compensator) could operate as a charge compensator for the positively charged E'_δ. But apparently it is not so. Rather than both types of defects increasing in tandem, their *nonsimultaneous* observability indicates anticorrelation: The E'_δ centers seem to emerge at the expense of Al E' defects. One possibility for the disappearance of Al E' centers upon annealing is through exchange, i.e., electron transfer from the ESR-active Al E' to a $[AlO_4]^+$ precursor, the latter now becoming paramagnetic.

In this context, we may also refer to the various other ESR works reporting the co-observation of Al-related defects in studies of E'-type centers in quartz.[17,73,74,76,80,84,85] For one, Buscarino *et al.* in their work[85] on the E'_δ in v-SiO_2 suggested a correlation between the E'_δ and E'_γ activation and the presence of $[AlO_4]^0$ centers, in the sense of hole transfer during thermal treatment ($T \gtrsim 500\,^\circ$C) from $[AlO_4]^0$ to diamagnetic E' precursors. Such limited correlation was previously concluded[80] to exist between the production of the E'_1 centers and the $[AlO_4]^0$ concentration, though repeatedly adding that the E'_1 production may be more complex than simple hole transfer.

In these schemes discussing the correlated presence of Al-related defects and E' center activation, the key influence of charge compensators has emerged.[73,74,80] In an archival work, the aspect of charge transfer between negatively charged $[AlO_4]^-$ and neutral AlO_3 entities upon irradiation, and correlated movement of charge compensators, has been demonstrated by Brower.[73,74] In this perspective, the essential point in co-observation of Al E' centers may be it bearing out the importance of charge compensators for E'_δ activation. If so, this may suggest the need to incorporate this complicating effect in correct theoretical atomic modeling of the defect, which is able to affect the unpaired spin-density distribution.[73]

Finally, in keeping with scientific objectivity, one may take a totally contrasting view, deferring any correlation: The ESR observation of Al E' centers might just constitute one more evidence for the E'_δ silica being O deficient,[74] an admitted requirement for a silica glass to enable E'_δ production. So, while the presence of Al impurities may not seem merely coincidental to E'_δ activation, understanding its precise correlative nature must await further detailed experimenting.

D. Lack of Si dimer (Si_2) ESR signal

With the E'_δ ESR signal decisively excluded as pertaining to the positively charged Si dimer (Si_2) defect, we (still) face the inconvenient situation that the latter center has so far not been experimentally observed, at least not recognized as such, unlike broad and concurring theoretical outcome, favoring the occurrence of this center as a *natural* defect in both crystalline[34–36,39,41] and amorphous[12,42,67] SiO_2. Upon hole trapping at the neutral O-vacancy precursor site ($O_3{\equiv}Si{-}Si{\equiv}O_3$) in c-SiO_2, the (calculated) probability for either ending up in Si_2 or E'_1 formation is calculated to be close, although the actual value may be somewhat uncertain.[34,40,41] As to a-SiO_2, it has been calculated that ~80% of the single O vacancies would remain in the dimer configuration upon hole trapping.[42] In illustrating the complexity of the point, the latter result has been countered in a later theoretical work[67] using an embedded-cluster method, expecting in a-SiO_2 a dimer concentration much less than that of Si dangling bond (DB) (E'_γ) configurations. Cautiously, the latter authors point out that predicting the ratio of defect types (dimer vs DB) formed at the specific network cited is very sensitive to the quantum-mechanical method employed in calculations. In any case, to a larger or lesser extent, Si dimer (Si_2) defects should occur in SiO_2, apparently in striking contrast with experimental facts. What then is the origin of this apparent paradox? Following are several considerations.

In a first view, it might simply result from the idea of unfavorable ESR signal properties, such as excessive line broadening, preventing Si_2 observation on pure experimental grounds. Yet, based on general ESR experimental experience with, and insight on, E'-type defects in SiO_2, this suggestion can hardly be retained.

Dealing with spectroscopic features, a second more far-fetched suggestion starts from the notion that the theoretically predicted ESR properties for the Si dimer (Si_2), such as, regarding g matrix and hf doublet splitting (yet not relative

hf structure intensity) comply with the experimental E'_δ properties. So, should the Si_2 defect persistently coexist only as a limited fraction (say $\lesssim$20%) of E'_δ, it will remain spectroscopically unrecognized, including, within current experimental error, what concerns the observed R_{hf} value—a case of inextricable signal overlap. In this context, we note that previous work[25] has suggested the existence of two E'_δ variants. Obviously, such overlap would result in effective lowering of the relative hf structure intensity ($n = 2$ for Si_2), so that the true R_{hf} value of E'_δ would be larger than actually measured. But then, of course, the question arises as to the case of E'_δ-silent silica only showing E'_1, E'_γ, and E'_α signals. Why does Si_2 also remain absent here?

This leads us to another possibility, based on calculated defect formation energies. Theoretical work on c-SiO_2 (α-quartz) concludes[34] that the formation of a positively charged Si dimer is, compared to that of E'_1, energetically unfavorable. So, E'_1 will be the dominant E'-type defect in (damaged) c-SiO_2. But apparently, while supported by one work,[41] it is contradicted by other theoretical works[40,42,67] on E'-type centers in a-SiO_2. Yet, in this respect, as cautioned by Mukhopadhyay *et al.*[67] we note that the accurate prediction of relative concentrations of possibly coexisting E'-type centers remains a key issue: It may still appear undecided.

But perhaps, in a contrary view, the Si_2 has already been observed: Indeed, as it stands today, the disproval of Si_2 as an E'_δ model has only been correctly established in commercial ^{60}Co γ-irradiated fused quartzes and perhaps, to a different extent,[21] in CVD-made silica subjected to x rays. Should, for example, dissimilar defect generation schemes (e.g., different types of samples, irradiation, etc.) result in generation of the supposedly two types of centers in different proportions, then unless ascertained by correct analysis of the ^{29}Si hf structure, one cannot be sure about the exact origin of the observed spectrum in terms of originating defect. It may all appear rather far-fetched, but if the anticipated highly isospectral appearances of E'_δ and Si_2 is correct, the utmost care is required, especially given the fact that the experimental situation is invariably aggravated by overlapping intense signals of other coexisting defects.

VI. CONCLUSIONS AND FINAL REMARKS

A multifrequency ESR study has been performed on E'-type point defects in amorphous silica, with the main focus on the E'_δ center, for which a trustworthy atomic model remains elusive. This has been carried out at both cryogenic and room temperatures using two types of ESR detection modes applied on six types of commercial vitreous silicas, subjected to three types of irradiations (UV, VUV, and ^{60}Co γ photons), with the intent to provide a consolidating expanded and statistically relevant set of data, over a broad range of ESR variables, on the ^{29}Si E'_δ hf structure—all aimed to further decisive atomic modeling. Much effort has been devoted to correct determination, by means of orthodox nonsaturation cw first-harmonic mode ESR spectroscopy, of the relative intensity $R_{hf}(\eta,n)$ of the associated ^{29}Si hf structure to the central Zeeman signal. The investigation has led to several results.

The E'_δ signal could be generated only in three types of a-silica, and only, yet always, by two types of irradiation, i.e., VUV and ^{60}Co γ rays. This suggests that E'_δ generation predominantly starts from preexisting sites where the signal "switching on" after irradiation with photons $h\nu > E_{g,SiO_2}$ (e-h pair generation) indicates, as key scenario, activation as a result of ionization rather than atom displacement processes. We further notice that, unlike VUV, the ^{60}Co γ-irradiation damaging requires an additional mild thermal step ($T_{an} = 320-345\,^\circ$C) to fully expose the E'_δ signal.

Apart from Si E'-type centers, Al-related defects were observed as well. Besides the "common" $[AlO_4]^0$ center, using second-harmonic saturation spectroscopy, the Al E' defect is revealed in as-γ-irradiated silica, but pertinently, only in those three showing the E'_δ center as well—bearing out these glasses to share structural and compositional aspects fit for common E'_δ and Al E' generation. Upon additional annealing, the E'_δ signal is seen to ramp up at the cost of the vanishing Al E'. While direct interdefect charge exchange is likely to be excluded, the correlated occurrence of both types of centers might suggest some indirect effect of Al-related centers in the E'_δ appearance. For one, it could signify some indirect role of charge compensators in activating and/or stabilizing E'_δ centers. The observation may inspire future work. However, in a contrasting view, the co-appearance of E'_δ and Al E' centers in the same glasses might just be seen as providing one more evidence that one is dealing with O-deficient a-silica, as admittedly required for the occurrence of E'_δ centers.

As a main result, the various R_{hf} values measured on the γ-irradiation KI-type a-silica are found reassuringly coinciding (within experimental error) over all observational frequencies and temperatures applied. The obtained average value ($R_{hf,av} \approx 20.3\%$) points to ^{29}Si hf interaction of the unpaired E'_δ electron with $n = 4(5)$ equivalent Si sites in a shell, herewith, in line with a previous result,[17] decisively refuting the repeatedly proposed positively charged Si-dimer (Si_2) model for the E'_δ center. The bare as-inferred value would plainly point to the $n = 4$ case, as initially proposed, yet it is felt that the $n = 5$ case cannot be excluded, and in fact is given full consideration, in view of previous experience with measurement of the ^{29}Si hf structure of Si DB-type defects.

In fact, according to current theoretical insight, none of the thus-far advanced atomic structures can be retained as a valuable candidate for the E'_δ defect. Basically, this is because the Si_4 and Si_5 models, like Si_2, essentially correspond to $n = 2$ or $n = 1$ cases as a result of the localization of the unpaired spin density to a large extent either in an elongated bond between a pair of Si atoms (Si_4), or primarily on a single Si atom (Si_5): The unpaired spin does not delocalize over the entire cluster; the reduction in symmetry of the electron wave function was attributed to the dynamic Jahn-Teller effect. Although E'_δ is widely accepted as a member of the specific O-vacancy-related E'-defect family, clearly this leaves a paradoxical situation.

As a corollary, attention is called for consistency in labeling, that is, the use of the E'_δ label, a defect spectrum observed by ESR, for the Si_2 model propagated by theory, should be discontinued: Si_2 is not E'_δ.

The E'_δ ESR signal parameters (such as g matrix, linewidth) as well as the hf structure are shown to be T-independent in the range $T = 4.2-300$ K, indicating that, should there be

involved any dynamical averaging process over electronically equivalent defect configurations, it must already be established at $T < 4.2$ K, putting strict limits on such a possibility. As the hf data reveal, neither does there occur any T-dependent redistribution of the unpaired electron orbital over adjacent atomic (Si) sites, all pointing to an electronically rigid structure. So, if E'_δ is admitted to be a delocalized electron center, it will concern a chemically fixed delocalized bonding (arrangement).

With the revealed incompatibility of the Si_2 model with the E'_δ center, it appears that we have reached the situation that over the numerous ESR studies carried out on SiO_2, the existence of the former has so far not been experimentally demonstrated, which, depending on one's view, may come as a surprise, for which several possibilities may be offered. As a tentative, perhaps naïve, one, the Si_2 defect may have escaped ESR detection because of its projected, closely isospectral ESR appearance as the E'_δ signal, so it may remain unresolved should it, for some unknown reason, only occur as a limited fraction of E'_δ. More possibilities have been discussed in the text.

Finally, in assessing the implications of the current work, more research will be required regarding modeling of E'_δ in vitreous SiO_2 and, correlated herewith, establishing, perhaps also experimentally, the fate of the anticipated Si_2 centers. As alluded to above, this research may be hampered by the very exceptional situation of dealing with two variants of defects showing highly isospectral ESR characteristics (apart, of course, from the respective R_{hf} values). It may inspire theoreticians to take another step in the demanding task of modeling of defects in a-SiO_2, that is, one taking into consideration additional complicating factors, such as the occurrence of charge compensators, dynamical averaging phenomena, and the influence of H.

ACKNOWLEDGMENTS

The authors would like to thank Duc A. P. Nguyen for assistance in ESR spectra simulation.

[1] M. L. Green, E. P. Gusev, R. Degraeve, and E. L. Garfunkel, J. Appl. Phys. **90**, 2057 (2001).
[2] D. L. Griscom, E. J. Friebele, K. J. Long, and J. W. Fleming, J. Appl. Phys. **54**, 3743 (1983).
[3] See, e.g., C. R. Helms and E. H. Poindexter, Rep. Prog. Phys. **57**, 791 (1994).
[4] R. A. Weeks, J. Appl. Phys. **27**, 1376 (1956).
[5] E. J. Friebele, G. H. Sigel, and D. L. Griscom, Appl. Phys. Lett. **28**, 516 (1976).
[6] Y. Hibino and H. Hanafusa, Appl. Phys. Lett. **45**, 614 (1984).
[7] D. L. Griscom and E. J. Friebele, Solid State Commun. **15**, 479 (1974).
[8] J. A. Weil, Phys. Chem. Miner. **10**, 149 (1984).
[9] R. A. Weeks, J. Non-Cryst. Solids **179**, 1 (1994); R. A. Weeks, R. H. Magruder III, and A. Stesmans, J. Non-Cryst. Solids **354**, 208 (2008).
[10] D. L. Griscom, in *Defects in SiO_2 and Related Dielectrics: Science and Technology*, NATO Science, Series II: Mathematical and Physical Chemistry, edited by G. Pacchioni, L. Skuja, and D. L. Griscom (Kluwer Academic, Dordrecht, 2000), p. 117.
[11] A. Stesmans, K. Clemer, and V. V. Afanas'ev, Phys. Rev. B **77**, 094130 (2008).
[12] B. R. Tuttle and S. T. Pantelides, Phys. Rev. B **79**, 115206 (2009).
[13] M. Zvanut, C. Benefield, and H. Hughes, IEEE Trans. Nucl. Sci. **41**, 2284 (1994).
[14] J. F. Conley, P. M. Lenahan, H. L. Evans, R. K. Lowry, and T. J. Morthorst, J. Appl. Phys. **76**, 2872 (1994).
[15] D. L. Griscom and E. J. Friebele, Phys. Rev. B **34**, 7524 (1986).
[16] S. P. Karna, H. A. Kurtz, A. C. Pineda, W. M. Shedd, and R. D. Pugh, in *Defects in SiO_2 and Related Dielectrics: Science and Technology*, NATO Science, Series II: Mathematical and Physical Chemistry (Ref. 10), p. 599.
[17] G. Buscarino, S. Agnello, and F. M. Gelardi, Phys. Rev. Lett. **94**, 125501 (2005).
[18] K. Vanheusden and A. Stesmans, J. Appl. Phys. **74**, 275 (1993).
[19] W. L. Warren, D. M. Fleetwood, M. R. Shaneyfelt, J. R. Schwank, P. S. Winokur, and R. A. B. Devine, Appl. Phys. Lett. **62**, 3330 (1993).
[20] W. L. Warren, D. M. Fleetwood, M. R. Shaneyfelt, P. S. Winokur, and R. A. B. Devine, Phys. Rev. B **50**, 14710 (1994).
[21] L. Zhang and R. G. Leisure, J. Appl. Phys. **80**, 3744 (1996).
[22] R. Tohmon, Y. Shimogaichi, Y. Tsuta, S. Munekuni, Y. Ohki, Y. Hama, and K. Nagasawa, Phys. Rev. B **41**, 7258 (1990).
[23] A. Stesmans, R. A. B. Devine, A. G. Revesz, and H. Hughes, IEEE Trans. Nucl. Sci. **37**, 2008 (1990).
[24] K. Vanheusden and A. Stesmans, Appl. Phys. Lett. **62**, 2405 (1993).
[25] A. Stesmans and K. Vanheusden, J. Appl. Phys. **76**, 1681 (1994).
[26] M. E. Zvanut, T. L. Chen, R. E. Stahlbush, E. S. Steigerwalt, and G. A. Brown, J. Appl. Phys. **77**, 4329 (1995).
[27] R. A. B. Devine, D. Mathiot, W. L. Warren, D. M. Fleetwood, and B. Aspar, Appl. Phys. Lett. **63**, 2926 (1993).
[28] R. A. B. Devine, D. Mathiot, W. L. Warren, and B. Aspar, J. Appl. Phys. **79**, 2302 (1996).
[29] A. Stesmans and V. V. Afanas'ev, Appl. Phys. Lett. **69**, 2056 (1996).
[30] D. L. Griscom, Phys. Rev. B **20**, 1823 (1979).
[31] T. E. Tsai and D. L. Griscom, J. Non-Cryst. Solids **91**, 170 (1987).
[32] J. R. Chavez, S. P. Karna, K. Vanheusden, C. P. Brothers, R. D. Pugh, B. K. Singaraju, W. L. Warren, and R. A. B. Devine, IEEE Trans. Nucl. Sci. **44**, 1799 (1997).
[33] S. P. Karna, A. C. Pineda, R. D. Pugh, W. M. Shedd, and T. R. Oldham, IEEE Trans. Nucl. Sci. **47**, 2316 (2000).
[34] K. C. Snyder and W. B. Fowler, Phys. Rev. B **48**, 13238 (1993).
[35] G. Pacchioni, G. Ieranò, and A. M. Márquez, Phys. Rev. Lett. **81**, 377 (1998).
[36] P. E. Blöchl, Phys. Rev. B **62**, 6158 (2000).
[37] S. Mukhopadhyay, P. V. Sushko, A. H. Edwards, and A. L. Shluger, J. Non-Cryst. Solids **345**, 703 (2004).
[38] Within experimental accuracy, no anisotropic contribution could so far be isolated from simulations of the observed powder patterns.
[39] A. C. Pineda and S. P. Karna, J. Phys. Chem. A **104**, 4699 (2000).
[40] N. Lopez, F. Illas, and G. Pacchioni, J. Phys. Chem. B **104**, 5471 (2000).

[41]M. Boero, A. Pasquarello, J. Sarnthein, and R. Car, Phys. Rev. Lett. **78**, 887 (1997).
[42]Z. Y. Lu, C. J. Nicklaw, D. M. Fleetwood, R. D. Schrimpf, and S. T. Pantelides, Phys. Rev. Lett. **89**, 285505 (2002).
[43]S. Mukhopadhyay, P. V. Sushko, V. A. Mashkov, and A. L. Shluger, J. Phys.: Condens. Matter **17**, 1311 (2005).
[44]H. Nishikawa, R. Nakamura, Y. Ohki, and Y. Hama, Phys. Rev. B **48**, 2968 (1993).
[45]L. N. Skuja, K. Kajihara, M. Hirano, and H. Hosono, Nucl. Instrum. Methods Phys. Res. B **266**, 2971 (2008).
[46]www.lightining.philips.com.
[47]www.almazoptics.com.
[48]www.heraeus-quartzglass.com.
[49]R. J. Powell and G. F. Derbenwick, IEEE Trans. Nucl. Sci. **NS18**, 99 (1971).
[50]T. Tatsumi, S. Fukuda, and S. Kadomura, Jpn. J. Appl. Phys. **33**, 2175 (1994).
[51]A. Stesmans, J. Magn. Reson. **76**, 14 (1988).
[52]A. Stesmans and Y. Wu, J. Phys. D: Appl. Phys. **21**, 1205 (1988).
[53]N. D. Yordanov and A. Christova, Appl. Magn. Reson. **6**, 341 (1994).
[54]G. Buscarino, S. Agnello, and F. M. Gelardi, Mod. Phys. Lett. **20**, 451 (2006).
[55]This dissonance may simply have arisen from inadvertent exchange in sample labeling, but otherwise immaterial for the current study.
[56]F. J. Feigl, W. B. Fowler, and K. L. Yip, Solid State Commun. **14**, 225 (1974); (b) J. K. Rudra and W. B. Fowler, **35**, 8223 (1987).
[57]D. L. Griscom, in *Glass: Science and Technology*, edited by D. R. Uhlmann and N. J. Kreidl (Academic, New York, 1990), p. 151.
[58]P. M. Lenahan and P. V. Dressendorfer, J. Appl. Phys. **55**, 3495 (1984).
[59]A. Kalnitsky, J. P. Ellul, E. H. Poindexter, P. J. Caplan, R. A. Lux, and A. R. Boothroyd, J. Appl. Phys. **67**, 7359 (1990).
[60]L. Lipkin, L. Rowan, A. Reisman, and C. K. Williams, J. Electrochem. Soc. **138**, 2050 (1991).
[61]S. T. Pantelides, Z. Y. Lu, C. Nicklaw, T. Bakos, S. Rashkeev, D. M. Fleetwood, and R. D. Schrimpf, J. Non-Cryst. Solids **354**, 217 (2008).
[62]V. V. Afanas'ev and A. Stesmans, J. Phys.: Condens. Matter **12**, 2285 (2000).
[63]R. H. Silsbee, J. Appl. Phys. **32**, 1459 (1961).
[64]D. L. Griscom, Nucl. Instrum. Methods Phys. Res. B **1**, 481 (1984).
[65]G. Buscarino, S. Agnello, and F. M. Gelardi, Phys. Rev. Lett. **97**, 135502 (2006).
[66]A. N. Trukhin, J. Troks, and D. L. Griscom, J. Non-Cryst. Solids **353**, 1560 (2007).
[67]S. Mukhopadhyay, P. V. Sushko, A. M. Stoneham, and A. L. Shluger, Phys. Rev. B **70**, 195203 (2004).
[68]A. H. Edwards and G. Germann, Nucl. Instrum. Methods Phys. Res. B **32**, 238 (1988).
[69]J. Vitko, J. Appl. Phys. **49**, 5530 (1978).
[70]H. Nishikawa, R. Nakamura, Y. Ohki, and Y. Hama, Phys. Rev. B **48**, 15584 (1993).
[71]L. N. Skuja, K. Kajihara, M. Hirano, A. Saitoh, and H. Hosono, J. Non-Cryst. Solids **352**, 2297 (2006).
[72]D. L. Griscom, Rev. Solid State Sci. **4**, 565 (1990).
[73]K. L. Brower, Phys. Rev. Lett. **41**, 879 (1978).
[74]K. L. Brower, Phys. Rev. B **20**, 1799 (1979).
[75]M. C. M. O'Brien, Proc. R. Soc. London, Ser. A **231**, 404 (1955).
[76]R. H. D. Nuttall and J. A. Weil, Can. J. Phys. **59**, 1696 (1981).
[77]R. Schnadt and A. Rauber, Solid State Commun. **9**, 159 (1971).
[78]H. Nishikawa, R. Nakamura, R. Tohmon, Y. Ohki, Y. Sakurai, K. Nagasawa, and Y. Hama, Phys. Rev. B **41**, 7828 (1990).
[79]T. E. Tsai, D. L. Griscom, and E. J. Friebele, Phys. Rev. Lett. **61**, 444 (1988).
[80]M. G. Jani, R. B. Bossoli, and L. E. Halliburton, Phys. Rev. B **27**, 2285 (1983).
[81]S.-T. Chang and S. A. Lyon, Appl. Phys. Lett. **48**, 136 (1986).
[82]K. L. Brower, Appl. Phys. Lett. **43**, 1111 (1983).
[83]A. Stesmans, J. Non-Cryst. Solids **179**, 10 (1994).
[84]J. Isoya, J. A. Weil, and L. E. Halliburton, J. Chem. Phys. **74**, 5436 (1981).
[85]G. Buscarino, S. Agnello, and F. M. Gelardi, Phys. Rev. B **73**, 045208 (2006).